Biochemical and Biophysical Research Communications 460 (2015) 151–156

Contents lists available at ScienceDirect

Biochemical and Biophysical Research Communications

journal homepage: www.elsevier.com/locate/ybbrc

Improving the osteointegration of Ti6Al4V by zeolite MFI coating

Yong Li [a], Yilai Jiao [b], Xiaokang Li [a], Zheng Guo [a, *]

[a] Department of Orthopedics, Xijing Hospital, Fourth Military Medical University, Xi'an, Shaanxi 710032, People's Republic of China
[b] Shenyang National Laboratory for Materials Science, Institute of Metal Research, Chinese Academy of Sciences, Shenyang, Liaoning 110016, People's Republic of China

ARTICLE INFO

Article history:
Received 8 February 2015
Available online 7 March 2015

Keywords:
Titanium alloy
Surface modification
Zeolites
Coating
Osteointegration

ABSTRACT

Osteointegration is crucial for success in orthopedic implantation. In recent decades, there have been numerous studies aiming to modify titanium alloys, which are the most widely used materials in orthopedics. Zeolites are solid aluminosilicates whose application in the biomedical field has recently been explored. To this end, MFI zeolites have been developed as titanium alloy coatings and tested *in vitro*. Nevertheless, the effect of the MFI coating of biomaterials *in vivo* has not yet been addressed. The aim of the present work is to evaluate the effects of MFI-coated Ti6Al4V implants *in vitro* and *in vivo*. After surface modification, the surface was investigated using field emission scanning electron microscopy (FE-SEM) and energy dispersive spectroscopy (EDS). No difference was observed regarding the proliferation of MC3T3-E1 cells on the Ti6Al4V (Ti) and MFI-coated Ti6Al4V (M–Ti) ($p > 0.05$). However, the attachment of MC3T3-E1 cells was found to be better in the M–Ti group. Additionally, ALP staining and activity assays and quantitative real-time RT-PCR indicated that MC3T3-E1 cells grown on the M–Ti displayed high levels of osteogenic differentiation markers. Moreover, Van-Gieson staining of histological sections demonstrated that the MFI coating on Ti6Al4V scaffolds significantly enhanced osteointegration and promoted bone regeneration after implantation in rabbit femoral condylar defects at 4 and 12 weeks. Therefore, this study provides a method for modifying Ti6Al4V to achieve improved osteointegration and osteogenesis.

1. Introduction

Titanium alloys are the most prevalent material used in orthopedic clinical practice because of their good biocompatibility and mechanical properties. However, there is still concern about the integration between titanium alloys and bone tissue (osteointegration) considering the inert nature of titanium alloys. Osteointegration is a crucial factor that affects the success of orthopedic implants. A typical example is the early loosening in hip or knee prostheses, which is a serious complication in total joint replacement [1]. If the osteointegration of an implant is unstable, the implant will experience micromotions that will activate the osteoclasts, leading to further implant loosening and finally implant failure [2]. To overcome this problem, titanium alloy surface modifications that focus on the surface morphology [3–6] and surface chemistry [7–10] are continuously being explored with the aim of achieving a stable integration between the bone and implant.

Zeolites are solid aluminosilicates with a uniform microporous structure and have been generally applied to catalysis, adsorption and ion exchange for commercial applications. Researchers have also widely investigated other potential applications for zeolites [11], which have shown great potential for biomedical applications [12]. Zeolites have been used as MRI contrast agents [13], antimicrobial coatings [14,15], drug delivery systems [16–19], and tissue engineering agents [20]. Recently, Seifu et al. demonstrated that fluorinated zeolites as novel oxygen vectors embedded in three-dimensional polyurethane scaffolds are capable of providing a sufficient oxygen supply to cells for tissue engineering [21]. Pellegrino et al. confirmed that zeolites can limit the negative effects caused by oxidative stress by adsorbing the reactive oxygen species [22]. Ninan et al. demonstrated that gelatin/hyaluronic acid (HA)/faujasite porous scaffolds can enhance wound healing by accelerating re-epithelization and collagen deposition [23].

Abbreviations: MFI, three letter code for zeolite nomenclature given by the International Zeolite Association; FE-SEM, field emission scanning electron microscopy; EDS, energy dispersive spectroscopy; Ti, Ti6Al4V; M-Ti, MFI coated Ti6Al4V.

* Corresponding author. Department of Orthopaedics, Xijing Hospital, Fourth Military Medical University, No. 127, West Chang Le Road, Xi'an, Shaanxi 710032, People's Republic of China. Fax: +86 29 84773411.
E-mail address: guozheng@fmmu.edu.cn (Z. Guo).

http://dx.doi.org/10.1016/j.bbrc.2015.02.157
0006-291X/

Among the different zeolites, Bedi et al. reported that the MFI zeolite can be synthesized on a titanium alloy surface as a coating to improve biocompatibility, corrosion resistance, osteoconductivity and osteoinductivity *in vitro* [24–26]. These studies showed that the MFI coating is a promising surface modification for titanium alloys. To the best of our knowledge, however, there have been no studies on the osteointegration of MFI coatings *in vivo*, which is important for orthopedic implants.

In this study, we investigated whether MFI-coated Ti6Al4V (M–Ti) exhibits greater biocompatibility and osteointegration compared with bare Ti6Al4V (Ti) substrates *in vitro* and *in vivo*. For this purpose, we created a MFI zeolite coating on a Ti6Al4V surface. The surface morphology, apatite formation ability, cell proliferation, surface cell morphology and cell osteogenic differentiation were investigated *in vitro*. We established a rabbit femur implant model to determine whether the MFI zeolite coating could improve the osteointegration and osteogenesis peri-implant.

2. Materials and methods

2.1. Substrate and MFI coating preparation

Medical Ti6Al4V (Shenyang National Laboratory for Materials Science) was used as the substrate. Disk-shaped samples (Ø12 mm × H2 mm) were used for *in vitro* assays, and cylindrical samples (Ø3 mm × L10 mm) were used for *in vivo* experiments. All of the samples were abraded with 2000-grit SiC paper and then cleaned with acetone (15 min), ethanol (15 min) and deionized water (15 min) in an ultrasonic bath.

The zeolite precursor solution was prepared by mixing tetrapropylammonium oxide (TPAOH, 50%), tetraethylorthosilicate (TEOS), and deionized water with a molar composition of TEOS: 0.2TPAOH:19.2H_2O, which was then heated for 4 h in an autoclave at 398 K. The samples were dipped into the obtained precursor solution for 2 h followed by air blowing for a few seconds and were subsequently dried in air for 12 h at 313 K.

A low-concentration synthesis solution was prepared by mixing TEOS, TPAOH and deionized water with a molar composition of TEOS: TPAOH: H2O = 1: 0.023: 178. In most cases, the samples were added to the above solution. The mixture was then transferred to a Teflon-lined stainless steel autoclave with a capacity of 500 ml. The autoclave was sealed and heated at 433 K for 0–48 h. After the hydrothermal treatments, the samples were washed thoroughly with hot water, dried at 373 K in air, and subsequently calcined at 823 K for 6 h to remove the organics from the zeolite framework.

2.2. Surface characterization

The morphology of the samples (Ti and M–Ti) was inspected by field emission scanning electron microscopy (FE-SEM, S-4800, HITACHI, Japan). An energy dispersive spectroscopic (EDS) analysis was performed to identify the chemical composition of the samples using EMAX. Prior to detection, the samples were sputtered with a thin layer of platinum (Pt) using a typical sputtering instrument to improve the surface conductivity.

2.3. Simulated body fluid (SBF) immersion experiments

The simulated body fluid (SBF) solution was prepared according to a previously described protocol [27], and the composition is presented in Table 1. The specimens were immersed in 15 ml of fresh SBF and incubated at 37 °C.The samples were removed from the water bath after 2 and 4 days, washed with deionized water twice and dried overnight in an air oven at 37 °C. FE-SEM (S-4800, HITACHI, Japan) was used to observe the apatite formation on the surface of the samples. The samples were sputtered with a thin layer of Pt to improve the surface conductivity.

Table 1
The ion concentration of SBF.

Ion	Ion concentrations (mM)
Na^+	142.0
K^+	5.0
Mg^{2+}	1.5
Ca^{2+}	2.5
Cl^-	147.8
HCO_3^-	4.2
HPO_4^{2-}	1.0
SO_4^{2-}	0.5
pH	7.40

2.4. Cell culture

Mouse preosteoblast cells (MC3T3-E1) were cultured in α-MEM medium supplemental with 10% fetal bovine serum (FBS, Gibco), 100U ml^{-1} penicillin and 100ug ml^{-1} in a humidified incubator at 37 °C with 5% CO_2. The medium was changed every 2 days.

2.5. Cell proliferation and morphology

MC3T3-E1 cells were seeded on the samples (Ti and M–Ti) at a density of 2 × 10^4/well in 24-well culture plates and cultured for 1, 4 and 7 days to evaluate the cell proliferation using Cell Count Kit-8 (CCK-8, Dojindo, Japan). Briefly, at each time point, the samples were transferred to new 24-well culture plates. Then, CCK-8 solution with a 10% volume of the medium was added to the wells, and the samples were incubated at 37 °C for 1 h. Next, 100 μl of the reaction solution was transferred into a new 96-well plate, and the optical density was measured at 450 nm using a microplate reader.

After incubation for 2 days, the samples were washed with PBS and fixed in 2.5% v/v glutaraldehyde at 4 °C overnight. The samples were then dehydrated through an ethanol series, critical-point dried and sputtered with Pt. The samples were observed using FE-SEM (S-4800, HITACHI, Japan).

2.6. Alkaline phosphatase (ALP) staining and activity assay

MC3T3-E1 cells were seeded on Ti and M–Ti samples at a density of 2 × 10^4/well in 24-well culture plates. After cell adherence, the cells were cultured using osteogenic medium (complete medium supplemented with 50 mg/L ascorbic acid, 10^{-8} M dexamethasone and 10 mM β-glycerol phosphate). The medium was changed every 2 days. After osteogenic medium treatment for 4 days and 7 days, the samples were stained with a BCIP/NBT alkaline phosphatase color development kit (Beyotime) according to the manufacturer's instructions. Images were captured with a zoom-stereo microscope. To determine the alkaline phosphatase (ALP) activity, the samples were washed twice with PBS and disrupted by freezing at −80 °C for 20 min with PBS containing 0.1% Triton X-100. Enzyme activity was detected using a commercially available kit (Beyotime), according to the manufacturer's instructions. The protein content was determined with a BCA kit (Thermo Scientific), and the alkaline phosphatase activity was expressed in arbitrary units per microgram of protein content.

2.7. Quantitative real-time RT-PCR

After osteogenic medium treatment for 7 and 14 days, the expressions of runt-related transcription factor-2 (Runx2), osteocalcin

(OCN), osteopontin (OPN) and collagen type-1 (Col-1) were determined to evaluate the differentiation of the cultured cells. Total RNA was extracted from cells cultured on the samples using the TRIzol reagent (Invitrogen Life Technologies) at each time point and subsequently converted into cDNA using PrimeScript™ RT Master Mix (Takara). Real-time PCR reactions were performed using SYBR Premix Ex Taq™ II (Takara) with the CFX96™ PCR System (Bio-Rad). β-actin was used as a housekeeping gene. The primers are shown in Table 2.

2.8. Animal experiments

For the *in vivo* experiments, Ti and M–Ti were implanted into the lateral femoral epicondyle of male New Zealand white rabbits with an average weight of 2.5–3.5 kg (n = 6 in each group). The surgical procedures were performed as previously described. The rabbits were anesthetized with phenobarbital sodium via intravenous injection. After shaving and sterilizing the surgical areas, an incision of approximately 2 cm was made to expose the lateral femoral epicondyle. Then, a cylindrical defect (diameter: 3 mm; length: 10 mm) was drilled on the lateral femoral epicondyle. Different samples were inserted into the predrilled defects; the incisions were then closed with sutures, and the surgical area was sterilized again. To prevent wound infection, each animal was given 40000 U penicillin per day via intramuscular injection for 3 days after surgery. All experimental procedures were approved by the ethics committee of the Fourth Military Medical University, according to the relevant guidelines and regulations.

2.9. Histological analysis

After implantation for 4 and 12 weeks, the rabbits were sacrificed by an intravenous injection of air under anesthesia. The femora condyle samples were harvested and fixed immediately with 4% paraformaldehyde buffer in PBS for 7 days. The samples were dehydrated in graded ethanol solutions from 70% to 100% and finally embedded in methyl methacrylate (MMA). The embedded samples were sliced (approximately 50 μm in thickness) using a modified interlocked diamond saw (Leica Microtome, Wetzlar, Germany) and stained with 1.2% trinitrophenol and 1% acid fuchsin (Von-Gieson staining). A qualitative analysis of bone formation was performed with a standard light microscope (Leica LA Microsystems, Bensheim, Germany) and a digital image analysis system (Image-Pro Plussoftware, Silver Spring, USA). The bone-to-implant interfacial interaction (BIC) and bone area (BA) were calculated based on Van-Gieson staining and were statistically analyzed. The bone area (BA) was defined as the area percentage of newly formed bone within a circle of 0.1 mm around the implant to the whole area.

2.10. Statistical analysis

The results were presented as the means ± SEM for each group. A one-way ANOVA followed by Bonferroni's multiple comparison tests were used to perform the statistical analysis. P-Values<0.05 was considered statistically significant.

Table 2
Primers used in real time PCR.

Gene	Forward primer sequence (5′- 3′)	Reverse primer sequence (5′- 3′)
β-actin	GGACTATGACTTAGTTGCGTTAC	TTTGCATTACATAATTTACACGA
Runx2	GAACCAAGAAGGCACAGACAGA	GGCGGGACACCTACTCTCATAC
ALP	TTGGGCAGGCAAGACACA	GAAGGGAAGGGATGGAGGAG
OCN	ACCATCTTTCTGCTCACTCTGCT	CCTTATTGCCCTCCTGCTTG
OPN	TACGACCATGAGATTGGCAGTGA	TATAGGATCTGGGTGCAGGCTGTAA
Col-1	GACATGTTCAGCTTTGTGGACCTC	GGGACCCTTAGGCCATTGTGTA

3. Results

3.1. Characterization

The SEM images showed that a polycrystalline MFI zeolite coating was successfully synthesized on Ti (Fig. 1A). The elemental transition was confirmed by EDS. After the surface modification, the EDS data showed that the surface was primarily composed of Si and O (Fig. 1A).

Large variations were observed between the Ti and M–Ti in terms of apatite formation. There was little apatite crystal formation on the M–Ti at 2 days, whereas no apatite was observed on the Ti surface (Fig. 1B). At later time points, the apatite formation on the M–Ti increased significantly. At 4 days, the M–Ti surface was almost completely covered by apatite, but there was still no apatite on the Ti surface at 4 days (Fig. 1B). These results indicate that M–Ti had better apatite-forming ability.

3.2. Cell proliferation and morphology

Cell proliferation was evaluated by the CCK-8 assay and was found to increase with increasing incubation time for both the Ti and M–Ti groups (Fig. 2A). Although there was no significant difference between the Ti and M–Ti, the OD values were higher in the M–Ti group at 4 and 7 days ($p > 0.05$, Fig. 2A).

The morphology of the cells on the materials was observed by FE-SEM. SEM images showed that the cells spread well on the surfaces of both the Ti and M–Ti (Fig. 2B). Moreover, the cells in the M–Ti group displayed more filopodia extensions compared with the Ti group (Fig. 2B), suggesting that the MFI coating promotes cell migration.

3.3. ALP staining and activity assay

The images of the ALP staining indicated that there were more positive cells on the M–Ti substrates at 4 and 7 days (Fig. 3A). The ALP activity assay was performed at the same time points. As the incubation time increased, the ALP activity increased in both groups. Moreover, the M–Ti group showed significantly higher ALP activity compared to the Ti group at 4 days (13.44 ± 1.132 vs. 8.244 ± 0.3792) and 7 days (17.00 ± 1.181 vs. 10.63 ± 1.553, $p < 0.05$, Fig. 3B).

3.4. Quantitative real-time RT-PCR

Cell differentiation was assessed at 7 and 14 days using osteogenic markers, including Runx2, OCN, OPN and Col-1, by quantitative real-time RT-PCR. The levels of Col-1 gene expression from the M–Ti group were significantly higher compared with those of the Ti group at 7 and 14 days ($p < 0.05$, Fig. 3C). There was no significant difference for Runx2, OCN or OPN gene expression at 7 days between the M–Ti and Ti groups; although their gene expressions were significantly higher in the M–Ti group at 14 days ($p < 0.05$, Fig. 3C). These results indicate that the MFI coating on the scaffolds promoted osteogenic differentiation in the MC3T3-E1 cells.

3.5. Histological analysis

Histological analysis based on Van-Gieson staining was used to assess the osteointegration and osteogenesis of the Ti and M–Ti implants. The results showed that the BIC increased with time for

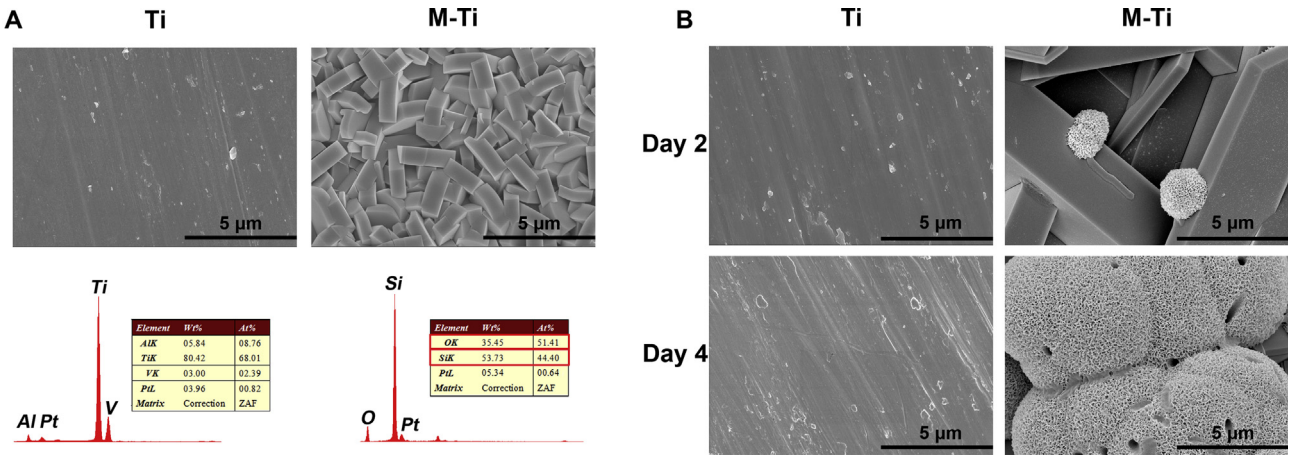

Fig. 1. SEM images of the surface morphology of Ti and M–Ti and the surface composition of Ti and M–Ti (A). SEM images of Ti and M–Ti after SBF immersion treatment.

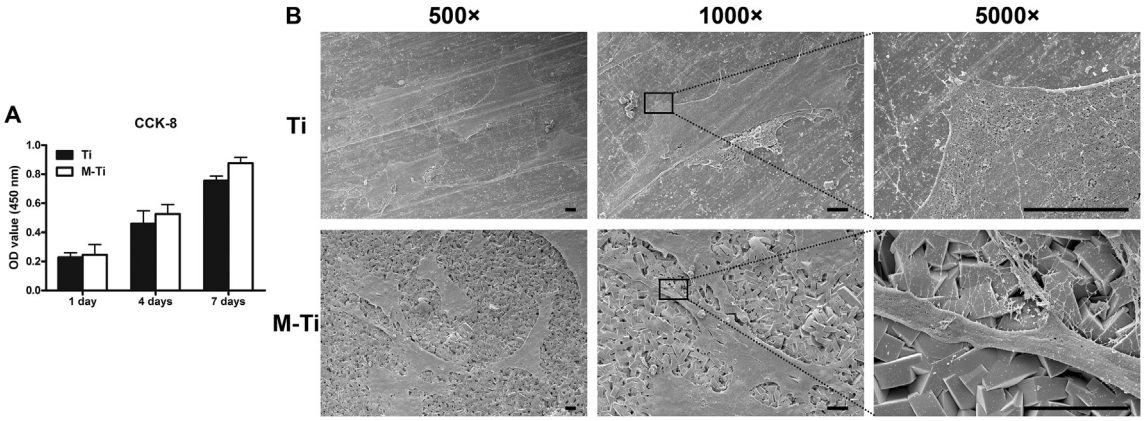

Fig. 2. Cell proliferation of MC3T3-E1 cells on different substrates (A) (n = 3, $p > 0.05$). Cell morphology on different substrates at 2 days (B). (Scale bar = 100 μm).

both groups (Fig. 4B) and that the BIC was significantly higher in the M–Ti group compared with the Ti group at 4 and 12 weeks ($p < 0.05$, Fig. 4B). The M–Ti group also showed better integration at both 4 and 12 weeks.

The bone area (BA) increased with increasing implantation time (Fig. 4A). Notably, histomorphometric analysis revealed that the BA was significantly higher in the M–Ti group compared with the Ti group at 4 and 12 weeks (Fig. 4C). The above results imply that the MFI coating improved the osteointegration and osteogenesis properties.

4. Discussion

Osteointegration plays an important role in the prognosis of bone-interfacing materials or devices, with improved osteointegration leading to a more stable implant and improved implant success. Although titanium alloys are widely used in clinical practice, problems still remain with regard to osteointegration. In recent decades, numerous studies have sought to modify titanium alloys to improve the osteointegration driven by cell–implant interactions at the implant surface [28–30]. Zeolites were initially used in the manufacturing industry, but researchers have demonstrated the value of zeolites in the bio-medical field as well. Among the zeolites, Bedi et al. found that MFI coatings can prevent the corrosion of titanium alloy while enhancing hFOB cell proliferation and osteogenic differentiation *in vitro* [24–26]. However, thus far, there have been no studies on the effects of this coating *in vivo*.

In this study, an MFI coating on a Ti6Al4V substrate was produced using the in situ crystallization method. SEM and EDS results verified the expected changes in surface morphology and composition, indicating successful synthesis of the MFI coating (Fig. 1A). The SBF immersion test is generally used to predict the *in vivo* bioactivity of different materials. After the immersion test, SEM images demonstrated that there was no apatite formation on the Ti6Al4V substrates at 2 or 4 days, whereas apatite formation was observed on the M–Ti substrates at 2 days, with a further increase at 4 days (Fig. 1B). These results suggest that the M–Ti had better *in vivo* bioactivity. The biocompatibility was investigated via the proliferation of MC3T3-E1 cells using the CCK-8 assay. Although the cell proliferation was not significantly different, the M–Ti group showed higher values (Fig. 2A). These results further indicate that the M–Ti group had a biocompatibility equal to that of Ti6Al4V. The adhesion and morphology of cells on the samples were investigated by SEM. The cells spread well on the surfaces of both the Ti and M–Ti (Fig. 2B). Moreover, the cells from the M–Ti group displayed more filopodia extensions than the Ti group (Fig. 2B), suggesting that the MFI coating promotes cell adhesion and migration.

In addition to cell adhesion and proliferation, cell differentiation was also investigated in our study. ALP staining and activity were evaluated at 4 and 7 days. The staining and activity assays were consistent, showing that the MFI coating upregulated ALP expression (Fig. 3A, B), which is an osteogenic differentiation marker. Furthermore, the mRNA expressions of osteoblast-related genes (Runx2, OCN, OPN and Col-1) were detected by quantitative real-

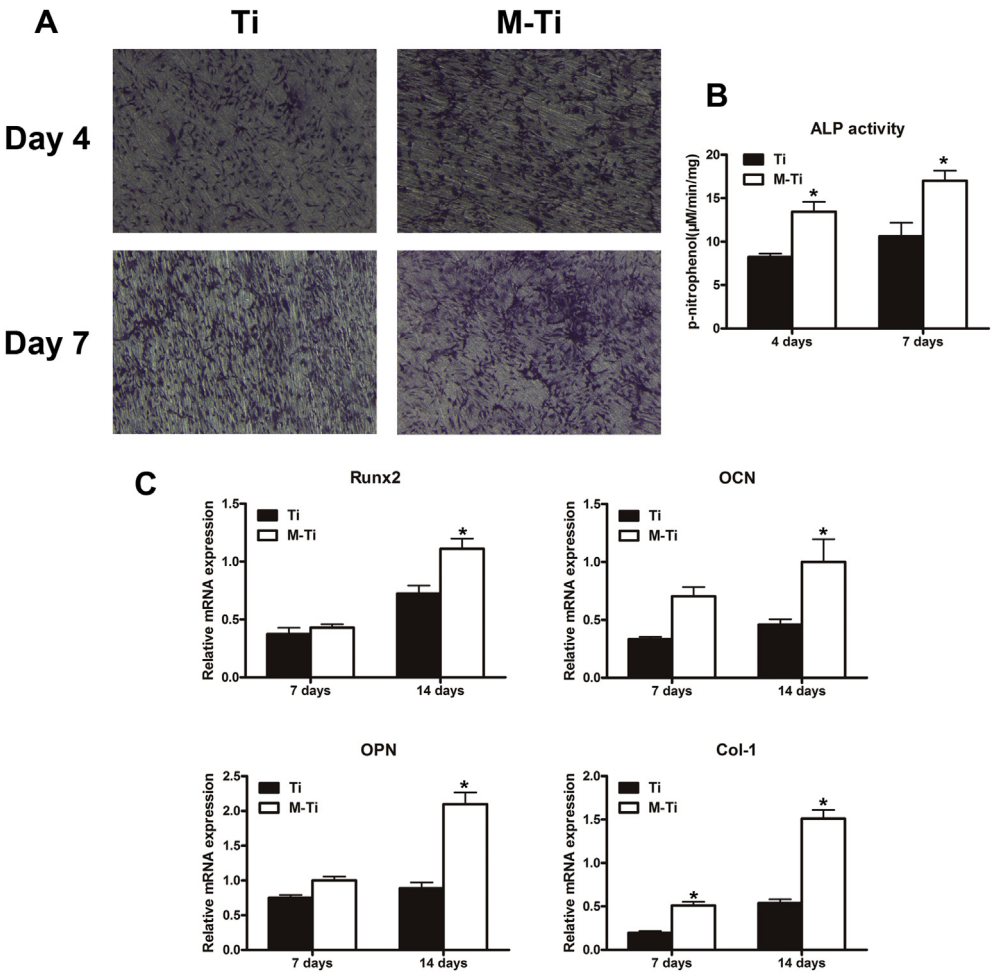

Fig. 3. Images of ALP staining at 4 and 7 days (A) and ALP activity for the different groups (B). Relative mRNA expression of Runx2, OCN, OPN and Col-1 (C). (* indicates statistical significance $p < 0.05$ vs. Ti.).

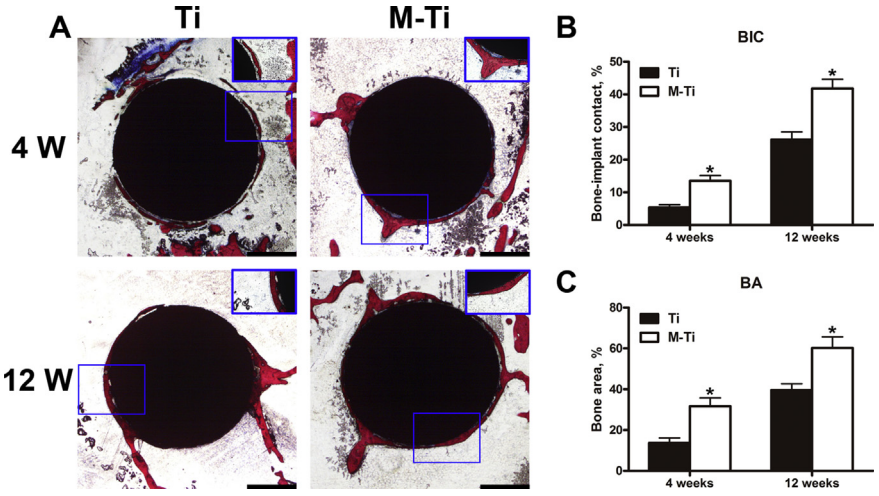

Fig. 4. Histological sections and histomorphometric analysis at 4 and 12 weeks post-operation. Histological images with Van Gieson staining for Ti and M–Ti (A). The tissue stained with a red color corresponds to newly formed bone. Analysis of the bone-implant contact (B) and bone area (C). (* indicates statistical significance $p < 0.05$ vs. Ti. Scale bar = 1000 μm). (For interpretation of the references to color in this figure legend, the reader is referred to the web version of this article.)

time RT-PCR to assess the differentiation of MC3T3-E1 cells. It was found that the levels of Col-1 gene expression were higher in the M–Ti group compared with those from the Ti group at both 7 and 14 days, whereas the levels of Runx2, OCN and OPN gene expression were higher in the M–Ti group only at 14 days (Fig. 3C). These results indicate that the MFI coating promotes the osteogenic differentiation of MC3T3-E1 cells *in vitro*. These *in vitro* results are consistent with those of previous studies [24–26].

A rabbit femoral condylar defect model was developed to investigate the osteointegration and osteogenesis properties *in vivo*. The BIC and BA were calculated based on Van-Gieson staining of histological sections. The BIC values indicated that the M–Ti group had better osteointegration than the Ti group at 4 and 12 weeks, and the BA values reflected active formation of new bone for the M–Ti group (Fig. 3A–C). These results are consistent with the *in vitro* findings, particularly the apatite formation ability test. The higher levels of osteointegration and osteogenesis found for the MFI coatings compared with the bare titanium alloy may be contributed to the surface microstructure provided by the zeolite crystals and the elemental composition of the zeolite [25].

Our results showed that the resulting MFI coating had a biocompatibility similar to that of the Ti6Al4V substrates, while displaying enhanced osteogenic differentiation of MC3T3-E1 cells *in vitro* and improved osteointegration and osteogenesis of the scaffolds *in vivo*. Thus, we have demonstrated that MFI coating is an effective method for modifying the surface of Ti6Al4V substrates. The underlying mechanism of the enhanced osteointegration and osteogenesis attained by the MFI coating is not yet clear. In future work, the biological mechanism requires further investigation.

In this study, MFI coatings were successfully fabricated on the surface of Ti6Al4V substrates. *In vitro* studies, including an apatite formation ability test, CCK-8 assay, cell morphology detection, ALP staining and activity test, and quantitative real-time RT-PCR, indicated that the MFI coating on Ti6Al4V scaffolds had good biocompatibility and promoted the adhesion and differentiation of MC3T3-E1 cells compared with bare Ti6Al4V substrates. Moreover, Van-Gieson staining of histological sections revealed that the M–Ti had greater osteointegration and osteogenesis properties *in vivo* than bare Ti6Al4V. Therefore, these functionalized Ti6Al4V substrates are promising for use in orthopedic applications.

Conflict of interest

None.

Acknowledgments

This work was supported by the Research Fund for the National Natural Science Foundation of China (No. 51271199), National Natural Science Foundation of China (No. 81171773) and Coordinative and Innovative Engineering Projects of Science and Technology of Shaanxi Province (No: 2012KTCG01-14). The authors thank AJE for the critical reading of the manuscript.

Transparency document

Transparency document related to this article can be found online at http://dx.doi.org/10.1016/j.bbrc.2015.02.157.

References

[1] T.W. Bauer, J. Schils, The pathology of total joint arthroplasty. I. Mechanisms of implant fixation, Skelet. Radiol. 28 (1999) 423–432.
[2] B. Mjoberg, The theory of early loosening of hip prostheses, Orthopedics 20 (1997) 1169–1175.
[3] K. Cai, J. Bossert, K.D. Jandt, Does the nanometre scale topography of titanium influence protein adsorption and cell proliferation? Colloids Surf. B Biointerfaces 49 (2006) 136–144.
[4] E.J. Kim, C.A. Boehm, A. Mata, et al., Post microtextures accelerate cell proliferation and osteogenesis, Acta Biomater. 6 (2010) 160–169.
[5] K.D. Jandt, Evolutions, revolutions and trends in biomaterials science – a perspective, Adv. Eng. Mater. 9 (2007) 1035–1050.
[6] M. Pegueroles, C. Aparicio, M. Bosio, et al., Spatial organization of osteoblast fibronectin matrix on titanium surfaces: effects of roughness, chemical heterogeneity and surface energy, Acta Biomater. 6 (2010) 291–301.
[7] S. Minagar, Y. Li, C.C. Berndt, et al., The influence of titania-zirconia-zirconium titanate nanotube characteristics on osteoblast cell adhesion, Acta Biomater. 12 (2015) 281–289.
[8] M. Kulkarni, A. Mazare, E. Gongadze, et al., Titanium nanostructures for biomedical applications, Nanotechnology 26 (2015) 062002.
[9] M. Mrksich, Using self-assembled monolayers to model the extracellular matrix, Acta Biomater. 5 (2009) 832–841.
[10] D.P. Liu, P. Majewski, B.K. O'Neill, et al., The optimal SAM surface functional group for producing a biomimetic HA coating on Ti, J. Biomed. Mater. Res. A 77 (2006) 763–772.
[11] C.M. Lew, R. Cai, Y. Yan, Zeolite thin films: from computer chips to space stations, Acc. Chem. Res. 43 (2010) 210–219.
[12] M. Danilczuk, K. Dlugopolska, T. Ruman, et al., Molecular sieves in medicine, Mini Rev. Med. Chem. 8 (2008) 1407–1417.
[13] E. Csajbok, I. Banyai, L. Vander Elst, et al., Gadolinium(III)-loaded nanoparticulate zeolites as potential high-field MRI contrast agents: relationship between structure and relaxivity, Chemistry 11 (2005) 4799–4807.
[14] N. Ninan, M. Muthiah, N.A. Bt Yahaya, et al., Antibacterial and wound healing analysis of gelatin/zeolite scaffolds, Colloids Surf. B Biointerfaces 115 (2014) 244–252.
[15] M. Neidrauer, U.K. Ercan, A. Bhattacharyya, et al., Antimicrobial efficacy and wound-healing property of a topical ointment containing nitric-oxide-loaded zeolites, J. Med. Microbiol. 63 (2014) 203–209.
[16] M. Spanakis, N. Bouropoulos, D. Theodoropoulos, et al., Controlled release of 5-fluorouracil from microporous zeolites, Nanomedicine 10 (2014) 197–205.
[17] A. Bertucci, H. Lulf, D. Septiadi, et al., Intracellular delivery of peptide nucleic acid and organic molecules using zeolite-L nanocrystals, Adv. Healthc. Mater. 3 (2014) 1812–1817.
[18] E. Khodaverdi, R. Honarmandi, M. Alibolandi, et al., Evaluation of synthetic zeolites as oral delivery vehicle for anti-inflammatory drugs, Iran. J. Basic Med. Sci. 17 (2014) 337–343.
[19] D. Krajisnik, R. Stepanovic-Petrovic, M. Tomic, et al., Application of artificial neural networks in prediction of diclofenac sodium release from drug-modified zeolites physical mixtures and antiedematous activity assessment, J. Pharm. Sci. 103 (2014) 1085–1094.
[20] L. Yu, J. Gong, C. Zeng, et al., Preparation of zeolite-A/chitosan hybrid composites and their bioactivities and antimicrobial activities, Mater. Sci. Eng. C Mater. Biol. Appl. 33 (2013) 3652–3660.
[21] D.G. Seifu, T.T. Isimjan, K. Mequanint, Tissue engineering scaffolds containing embedded fluorinated-zeolite oxygen vectors, Acta Biomater. 7 (2011) 3670–3678.
[22] P. Pellegrino, B. Mallet, S. Delliaux, et al., Zeolites are effective ROS-scavengers in vitro, Biochem. Biophys. Res. Commun. 410 (2011) 478–483.
[23] N. Ninan, M. Muthiah, I.K. Park, et al., Faujasites incorporated tissue engineering scaffolds for wound healing: in vitro and in vivo analysis, ACS Appl. Mater. Interfaces 5 (2013) 11194–11206.
[24] R.S. Bedi, D.E. Beving, L.P. Zanello, et al., Biocompatibility of corrosion-resistant zeolite coatings for titanium alloy biomedical implants, Acta Biomater. 5 (2009) 3265–3271.
[25] R.S. Bedi, L.P. Zanello, Y. Yan, Osteoconductive and osteoinductive properties of zeolite MFI coatings on titanium alloys, Adv. Funct. Mater. 19 (2009) 3856–3861.
[26] R.S. Bedi, G. Chow, J. Wang, et al., Bioactive materials for regenerative medicine: zeolite-hydroxyapatite bone mimetic coatings, Adv. Eng. Mater. 14 (2012) 200–206.
[27] T. Kokubo, H. Takadama, How useful is SBF in predicting in vivo bone bioactivity? Biomaterials 27 (2006) 2907–2915.
[28] J. Havlikova, J. Strasky, M. Vandrovcova, et al., Innovative surface modification of Ti-6Al-4V alloy with a positive effect on osteoblast proliferation and fatigue performance, Mater. Sci. Eng. C Mater. Biol. Appl. 39 (2014) 371–379.
[29] S. Zankovych, M. Diefenbeck, J. Bossert, et al., The effect of polyelectrolyte multilayer coated titanium alloy surfaces on implant anchorage in rats, Acta Biomater. 9 (2013) 4926–4934.
[30] C.J. Frandsen, K.S. Brammer, K. Noh, et al., Tantalum coating on TiO2 nanotubes induces superior rate of matrix mineralization and osteofunctionality in human osteoblasts, Mater. Sci. Eng. C Mater. Biol. Appl. 37 (2014) 332–341.